Available online at www.sciencedirect.com

ScienceDirect

Procedia Structural Integrity 9 (2018) 279–286

Structural Integrity Procedia

www.elsevier.com/locate/procedia

IGF Workshop "Fracture and Structural Integrity"

Effect of temperature and exploitation time on tensile properties and plain strain fracture toughness, K_{Ic}, in a welded joint

Ivica Čamagić[a], Simon Sedmak[b]*, Aleksandar Sedmak[c], Zijah Burzić[d], Mladen Marsenić[a]

[a]*Faculty of Technical Sciences, 7 Kneza Miloša Street, 38220 K. Mitrovica, Serbia*
[b]*Innovation Center of the Faculty of Mechanical Engineering, 16 Kraljice Marije Street, 11120 Belgrade, Serbia*
[c] *Faculty of Mechanical Engineering, 16 Kraljice Marije Street, 11120 Belgrade, Serbia*
[d] *Military Technical Institute, 2 Ratka Resanovića Street, 11000 Belgrade, Serbia*

Abstract

Effect of temperature and exploitation time on resistance to brittle fracture of welded joint constituents of new and 40 years exploited low-alloyed *Cr-Mo* steel *A*-387 *Gr. B* has been analysed. The plane strain fracture toughness is used as the measure of resistance to brittle fracture of base metal, weld metal and heat affected zone from both new and exploited. The stress-strain curves have been determined as well, to get better inside in welded joint behavior. Comparison of the results indicate detrimental effect of both temperature and exploitation time, both for tensile properties and for the resistance to brittle fracture.

Peer-review under responsibility of the Gruppo Italiano Frattura (IGF) ExCo.

Keywords: welded joint; tensile properties; plane strain fracture toighness; critical crack length

1. Introduction

A long-time exploitation period of a pressure vessel-reactor (over 40 years) has caused certain damages to the reactor mantle. The occurrence of these damages required a thorough inspection of the reactor construction itself, as well as the repair of damaged parts. Repairing of the reactor included the replacement of a part of the reactor mantle with newly built-in material. The pressure vessel was made of low-alloyed Cr-Mo steel A-387 Gr. B in accordance

* Corresponding author
E-mail address: simon.sedmak@yahoo.com

2452-3216
Peer-review under responsibility of the Gruppo Italiano Frattura (IGF) ExCo.
10.1016/j.prostr.2018.06.034

with ASTM standard with (0,8-1,15)% Cr and (0,45-0,6)% Mo. For designed working parameters (p = 35bar and t = 537°C) the material is in the area of tendency towards decarbonisation of the surface which is in contact with hydrogen. The surface decarbonisation may reduce the strength of the material and its resistance to brittle fratcure. The reactor, based on its construction represents a vertical pressure vessel with a cylindrical mantle. Testing of a new and exploited parent metal (PM), as well as the components of welded joints (weld metal- WM and heat affected zone (HAZ), low-alloyed steel from which the reactor was made, included determination of tensile properties of the new PM, WM and butt welded joint new PM-exploited PM and determination of fracture mechanics parameters of the new and exploited PM and welded joint components, at room and working temperature of 540°C, Čamagić (2013).

2. Materials for testing

Exploited PM was steel A-387 *Gr. B* with thickness of 102 mm, whereas the new PM was also made of steel A-387 *Gr. B* and with thickness of 102 mm. Chemical composition and mechanical properties of the exploited and new PM according to the attest documentation are given in tab. 1 and 2, Čamagić (2013).

Table 1. Chemical composition of exploited and new PM specimens

Specimen mark	% mas.							
	C	Si	Mn	P	S	Cr	Mo	Cu
E	0,15	0,31	0,56	0,007	0,006	0,89	0,47	0,027
N	0,13	0,23	0,46	0,009	0,006	0,85	0,51	0,035

Table 2. Mechanical properties of exploited and new PM specimens

Specimen mark	Yield stress, $R_{p0,2}$, MPa	Tensile strength, R_m, MPa	Elongation, A, %	Impact energy, J
E	320	450	34,0	155
N	325	495	35,0	165

Welding of steel sheets made of exploited and new PM was performed in two stages, according to the requirements given in the welding procedure provided by a welding specialist, and these stages include:

- Root weld by E procedure, using a coated LINCOLN S1 19G electrode (AWS: E8018-B2), and
- Filling by arc welding under powder protection (EPP), where wire denoted as LINCOLN LNS 150 and powder denoted as LINCOLN P230 were used as additional materials.

Chemical composition of the coated electrode LINCOLN S1 19G, and the wire LINCOLN LNS 150 is given in tab. 3, whereas their mechanical properties, are given in tab. 4, Čamagić (2013). Butt welded joint was made with a U-weld. The shape of the groove for welding preparation was chosen based on sheet thickness, in accordance with appropriate standards SRPS EN ISO 9692-1:2012 and SRPS EN ISO 9692-2:2008.

Table 3. Chemical composition of additional welding materials

Filler material	% mas.						
	C	Si	Mn	P	S	Cr	Mo
LINCOLN Sl 19G	0,07	0,31	0,62	0,009	0,010	1,17	0,54
LINCOLN LNS 150	0,10	0,14	0,71	0,010	0,010	1,12	0,48

Table 4. Mechanical properties of additional materials

Filler material	Yield stress, $R_{p0,2}$, MPa	Tensile strength, R_m, MPa	Elongation, A, %	Impact energy, J na 20°C
LINCOLN Sl 19G	515	610	20	> 60
LINCOLN LNS 150	495	605	21	> 80

3. Determination of tensile properties

Basic characteristics of material strength, as well as the stress-elongation curves required for stress analysis, are obtained by tensile testing. Tensile testing of butt welded joint at room temperature, including the shape and dimensions of specimens as well as the procedure itself are defined by SRPS EN 895:2008 standard,. This standard primarily defines transverse tension, i.e. introduction of the load transversely to the welded joint. Determination of tensile properties of PM is defined by SRPS EN 10002-1 standard. Unlike room temperature testing, the testing procedures at increased temperature of 540°C, as well as the specimen geometry are defined by SRPS EN 10002-5 standard.

Testing results of butt welded joint specimens by transverse tension at room temperature of 20°C and working temperature of 540°C are given in tab. 5, Čamagić (2013). Typical tensile stress-elongation curve for specimen of butt welded joint marked as ZS-1-1, tested at room temperature is shown in fig. 1, Čamagić (2013), and for specimen marked as ZS-2-1, tested at working temperature is shown in fig. 2, Čamagić (2013).

Table 5. Results of tensile testing of the welded joint

Specimen designation	Testing temperature, °C	Yield stress, $R_{p0,2}$, MPa	Tensile strength, R_m, MPa	Elongation[1], A, %	Fracture location
WJ-1-1		295	451	19,2	Expl. PM
WJ-1-2	20	285	448	20,4	Expl. PM
WJ-1-3		291	454	19,7	Expl. PM
WJ-2-1		217	293	26,3	Expl. PM
WJ-2-2	540	205	285	25,6	Expl. PM
WJ-2-3		211	287	26,9	Expl. PM

[1] measured at L0 = 100mm, as comparative value (not as a material property).

Testing results of specimens of the new PM at room temperature of 20°C and working temperature 540°C are given in tab. 6, Čamagić (2013). Testing of exploited PM was not performed, because during the testing of welded joint specimens all tested specimens fractured in the exploited PM, which provided us with the properties of exploited PM. typical tensile stress-elongation curve for specimen denoted by PM-1-1N, taken from the new PM and tested at room temperature is given in fig. 3, Čamagić (2013), and for specimen PM-2-1N, also taken from the new PM, but tested at working temperature, is shown in fig. 4, Čamagić (2013).

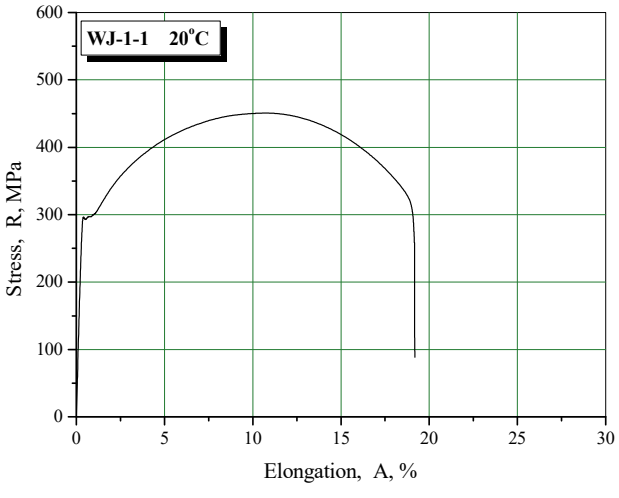

Fig. 1. Stress-elongation diagram of a welded joint specimen WJ-1-1.

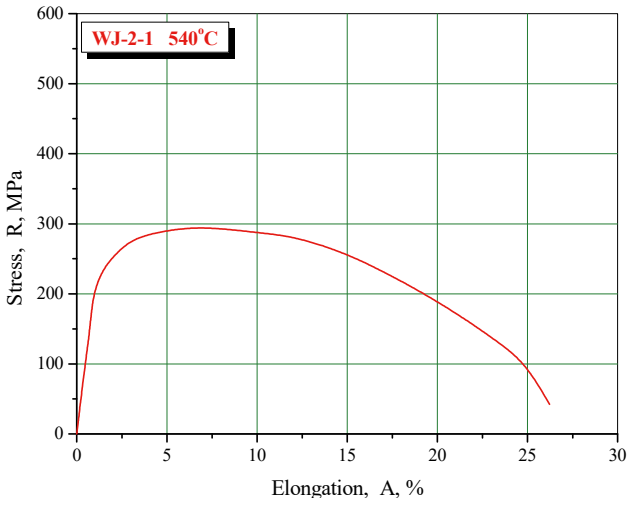

Fig. 2. Stress-elongation diagram of a welded joint specimen WJ-2-1.

Table 6. Results of tensile testing of new PM specimens

Specimen designation	Testing temperature, °C	Yield stress, $R_{p0,2}$, MPa	Tensile stress, R_m, MPa	Elongation, A, %
PM-1-1N	20	342	513	27,5
PM-1-2N		339	505	28,3
PM-1-3N		335	498	28,6
PM-2-1N	540	251	323	29,1
PM-2-2N		242	316	30,8
PM-2-3N		247	320	30,4

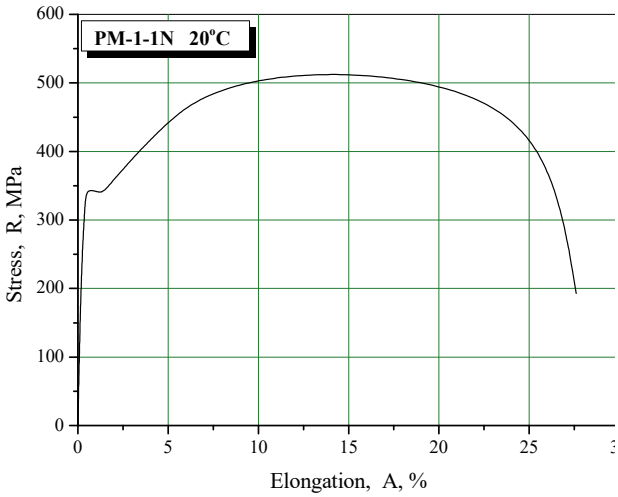

Fig. 3. Stress-elongation diagram for new PM specimen PM-1-1N.

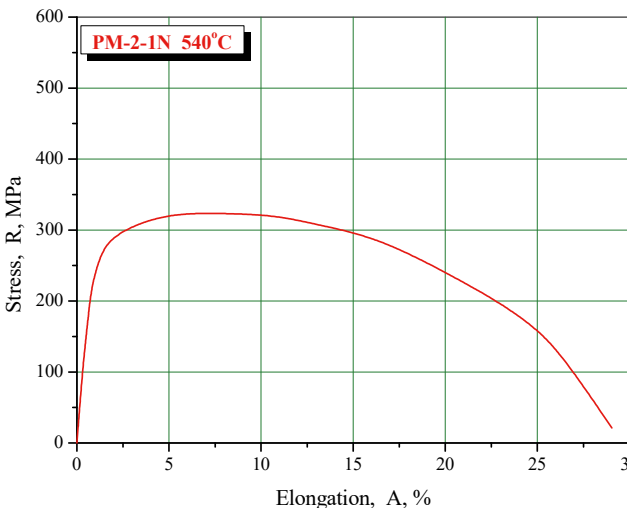

Fig. 4. Stress-elongation diagram for new PM specimen PM-2-1N.

Testing results of WM specimens tested at room temperature of 20°C and working temperature of 540°C are given in tab.7, Čamagić (2013). Typical tensile stress-elongation curve for WM specimen marked as WM-1-1, tested at room temperature is shown in fig.5, Čamagić (2013), and for specimen marked as WM-2-1, tested at working temperature is shown in fig. 6, Čamagić (2013).

Table 7. Results of tensile testing of WM specimens

Specimen designation	Testing temperature, °C	Yield stress, $R_{p0,2}$, MPa	Tensile strength, R_m, MPa	Elongation, A, %
WM-1-1	20	518	611	20,9
WM-1-2		510	597	22,7
WM-1-3		514	605	21,3
WM-2-1	540	331	419	26,1
WM-2-2		319	406	27,3
WM-2-3		325	412	27,7

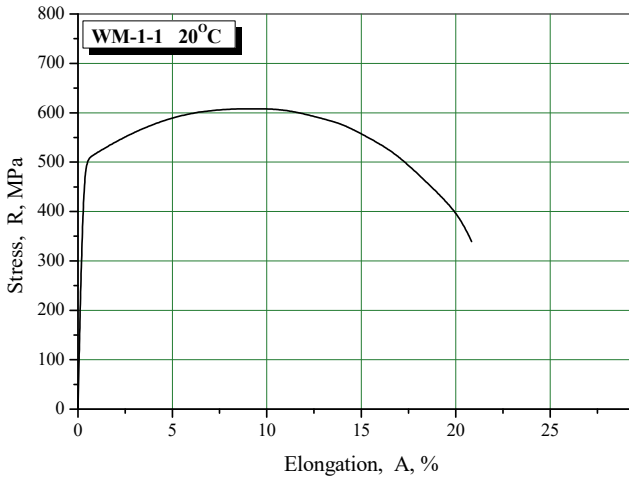

Figure 5. Stress-elongation diagram for WM specimen, WM-1-1.

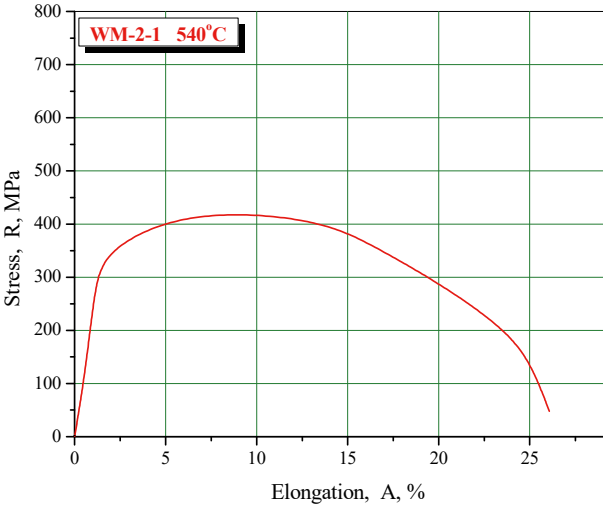

Figure 6. Stress-elongation diagram for WM specimen, WM-2-1.

4. Determination of plane strain fracture toughness, K_{Ic}

The impact of exploitation conditions, i.e. exploitation time and temperature on tendency to brittle fracture of the new and exploited PM, as well as the components of welded joint (WM and HAZ) was evaluated by determining the plane strain fracture toughness, that is, critical value of stress intensity factor, K_{Ic}. The testing was performed at room temperature of 20°C and working temperature of 540°C.

For determination of, K_{Ic}, at room temperature the three point bending specimen (SEB) were used, whose geometry is defined by ASTM E399, ASTM E399-89, and ASTM E1820 standards, ASTM E 1820-99a. For determination of K_{Ic} at working temperature of 540°C the modified CT tensile specimens were used, whose geometry is in accordance with BS 7448 Part 1, standard, BS 7448-Part 1. Fracture toughness, K_{Ic}, is determined indirectly through critical J-integral, J_{Ic}, using elastic-plastic fracture mechanics (EPFM) defined by ASTM E813, ASTM E813-89, ASTM E 1737, ASTM E 1737-96, ASTM E1820, ASTM E 1820-99a and BS 7448 Part 1 and 2, standards, that is, by monitoring the crack development in the conditions of plasticity. The experiments are carried out by the testing method of a single specimen by successive partial unload, i.e. by the single specimen permeability method, as defined by ASTM E813 standard.

Based on the obtained data, J-Δa curve is constructed on which the regression line is constructed according to ASTM E1152, ASTM E1152-91. From the obtained regression line the critical J-integral, J_{Ic}, is obtained. Knowing the value of critical, J_{Ic}, integral, the value of critical stress intensity factor or plane strain fracture toughness, K_{Ic}, can be calculated using the dependence:

$$K_{Ic} = \sqrt{\frac{J_{Ic} \cdot E}{1-\nu^2}} \tag{1}$$

Calculated values of critical stress intensity factor, K_{Ic}, are given in tab. 8 for notched specimens in new PM, and in tab. 9 for notched specimens in exploited PM, tested at room temperature of 20°C and working temperature of 540°C, Čamagić (2013). It is important to point out that in calculation of plane strain fracture toughness, K_{Ic}, one value was used for elastic modulus at room temperature (210GPa) and other value for increased temperatures (approximately 160GPa for 540^{0}C). By applying basic formula of fracture mechanics:

$$K_{Ic} = \sigma \cdot \sqrt{\pi \cdot a_c} \tag{2}$$

and by introducing the values of conventional yield stress, $R_{p0,2} = \sigma$, [1, 17], the approximate values for critical crack length, a_c , can be calculated.

Table 8. Values of K_{Ic} notched specimens in new PM

Specimen mark	Testing temperature, °C	Critical J-integral, J_{Ic}, kJ/m^2	Critical stress intensity factor, K_{Ic}, MPa m$^{1/2}$	Critical crack length, a_c, mm
PM-1-1n	20	60,1	117,8	38,5
PM-1-2n		63,9	121,4	40,8
PM-1-3n		58,6	116,3	37,5
PM-2-1n	540	43,2	87,2	40,0
PM-2-2n		44,7	88,7	41,4
PM-2-3n		45,3	89,2	41,9

Table 9. Values of K_{Ic} notched specimens in exploited PM

Specimen mark	Testing temperature, °C	Critical J-integral, J_{Ic}, kJ/m^2	Critical stress intensity factor, K_{Ic}, MPa m$^{1/2}$	Critical crack length, a_c, mm
PM-1-1e	20	47,8	105,0	41,7
PM-1-2e		42,1	98,6	36,8
PM-1-3e		40,7	96,9	35,6
PM-2-1e	540	24,5	65,6	30,8
PM-2-2e		22,7	63,2	28,6
PM-2-3e		21,8	61,9	27,4

The characteristic diagrams *F-δ*, and *J-Δa* for specimen taken out from the sample of new PM are given in fig. 7 for specimen marked as PM-1-1n tested at room temperature, and in fig. 8 for specimen marked as PM-2-1n tested at the temperature of 540°C, Čamagić (2013). Diagrams *F-δ*, and *J-Δa* for specimens of exploited PM WM and HAZ from the side of new PM and HAZ from the side of exploited PM, tested at room and working temperature, due to the scope of the paper are not presented, Čamagić (2013).

Calculated values of critical stress intensity factor, K_{Ic}, and critical crack length, a_c, are given in the tab.10 for notched specimens in WM, tested at room temperature of 20°C and working temperature of 540°C, Čamagić (2013).

Calculated values of critical stress intensity factor, K_{Ic}, and critical crack length, a_c, are given in the tab. 11 for notched specimens in HAZ from the side of the new PM and in tab. 12 for notched specimens in HAZ from the side of the exploited PM, tested at room temperature of 20°C and working temperature of 540°C, Čamagić (2013).

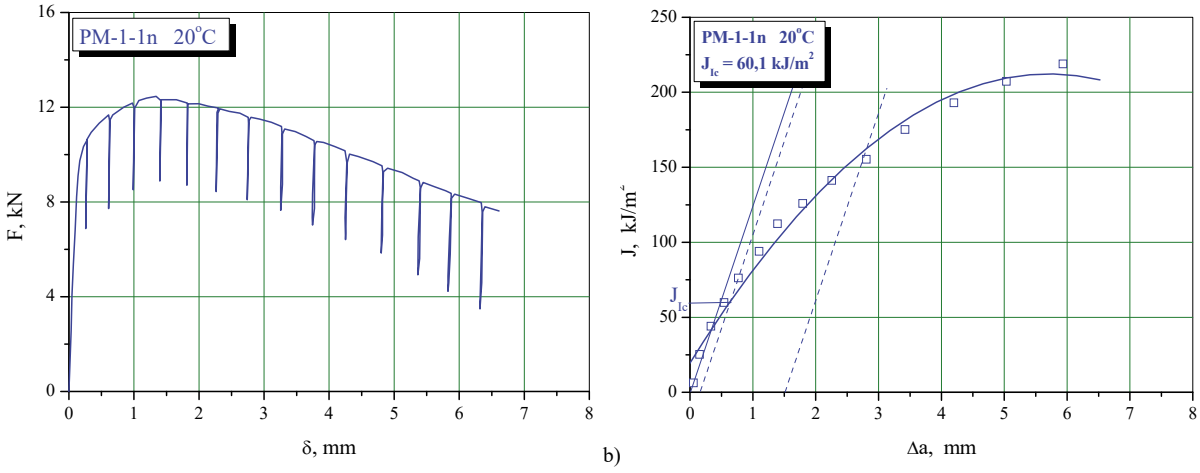

Fig. 7. Diagrams F-δ (a) and J-Δa (b) of the specimen PM-1-1n.

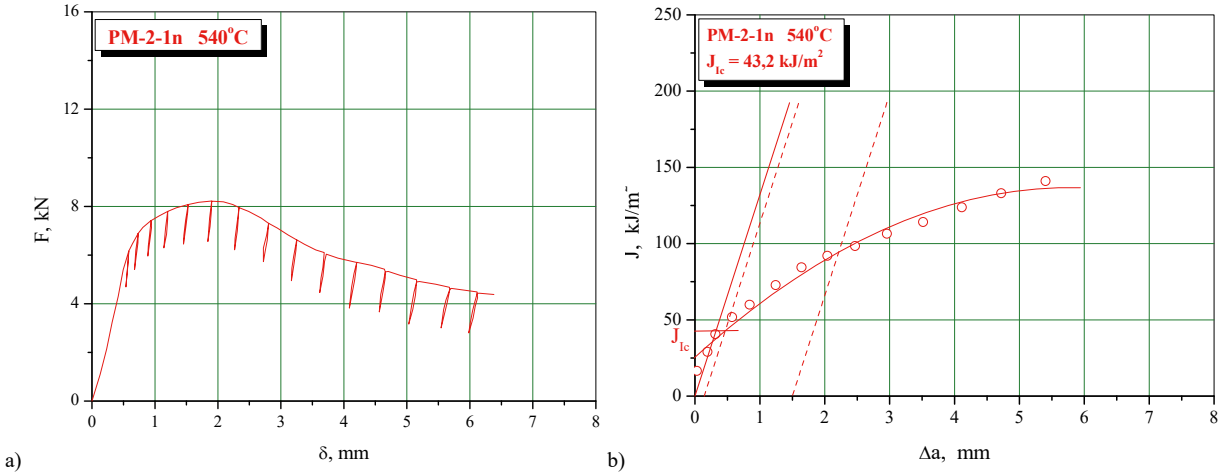

Fig. 8. Diagrams F-δ (a) and J-Δa (b) of the specimen PM-2-1n.

Table 10. Values of K_{Ic} notched specimens at WM

Specimen mark	Testing temperature, °C	Critical J-integral, J_{Ic}, kJ/m^2	Critical stress intensity factor, K_{Ic}, MPa m$^{1/2}$	Critical crack length, a_c, mm
WM-1-1	20	72,8	129,6	20,2
WM-1-2		74,3	130,9	20,7
WM-1-3		71,1	128,1	19,8
WM-2-1	540	50,2	93,9	17,4
WM-2-2		52,6	96,2	18,2
WM-2-3		48,4	92,2	16,8

Table 11. Values of, K_{Ic} notched specimens at new HAZ

Specimen mark	Testing temperature, °C	Critical J-integral, J_{Ic}, kJ/m^2	Critical stress intensity factor, K_{Ic}, MPa m$^{1/2}$	Critical crack length, a_c, mm
HAZ-1-1n	20	53,6	111,2	34,3
HAZ-1-2n		51,7	109,2	33,0
HAZ-1-3n		49,8	107,2	31,8
HAZ-2-1n	540	33,6	76,9	31,1
HAZ-2-2n		34,2	77,5	31,6
HAZ-2-3n		36,1	79,7	33,4

Table 12. Values of, K_{Ic} notched specimens at exploited HAZ

Specimen mark	Testing temperature, °C	Critical J-integral, J_{Ic}, kJ/m^2	Critical stress intensity factor, K_{Ic}, MPa m$^{1/2}$	Critical crack length, a_c, mm
HAZ-1-1e	20	42,4	96,3	32,0
HAZ-1-2e		36,1	91,3	31,5
HAZ-1-3e		35,6	90,6	31,1
HAZ-2-1e	540	20,2	59,6	25,4
HAZ-2-2e		22,5	62,9	28,3
HAZ-2-3e		21,7	61,8	27,3

5. Discussion and conclusions

The obtained results of testing the welded joint specimens by introducing load transversely to welded joint, tab. 5, indicate that all tested specimens have cracked in exploited PM, indicating significant weakening of exploited PM. Character of obtained tensile curves at room temperature corresponds to a ductile material with approximate share of homogeneous and non-homogeneous elongation at a ratio of 1/2:1/2. When testing the welded joint specimens at working temperature the ratio of homogeneous to non-homogeneous elongation is approximately 1/4:3/4, which is rather unfavourable. Based on the obtained testing results of specimens taken from the new and exploited PM, WM and HAZ from the side of the new and exploited PM, it can be seen that with the increase of the testing temperature there is a decrease in the value of critical J_{Ic}, integral, that is, fracture toughness, K_{Ic}. The value of critical crack length, a_c, also decreases.

Based on the testing results of tensile properties of specimens taken from the welded joint of the new PM and WM, it can be concluded that increased temperature reduces strength properties, but increases elongation. The increase of elongation with the temperature increase is explained by the increased overall plasticity of the material at higher temperatures, but also by the significantly unfavorable ratio of homogenous and non-homogenous elongation. Also, the exploitation time significantly impacts the reduction of strength properties and strain properties, which can be related to the microstructures of the exploited and new PM, as presented by Čamagić (2013). Based on the obtained testing results of the critical stress intensity factor K_{Ic}, determined indirectly through the critical J_{Ic} integral, one can conclude that the lowest resistance to the crack propagation, not surprisingly, belongs to HAZ, whereas the highest resistance to crack propagation, somewhat surprisingly, belongs to WM.

6. Acknowledgements

Parts of this research were supported by the Ministry of Sciences and Technology of Republic of Serbia through the Grant OI 174001 “Dynamics of hybrid systems with complex structures”.

References

ASTM E 1290-89, Standard Test Method for Crack-Tip Opening Displacement (CTOD) Fracture Toughness Measurement, Annual Book of ASTM Standards, Vol. 03.01, 1993.

ASTM E 1737-96, Standard Test Method for J Integral Characterization of Fracture Toughness, Annual Book of ASTM Standards, Vol.03.01., 1996.

ASTM E 1820-99a, Standard Test Method for Measurement of Fracture Toughness, Annual Book of ASTM Standards, Vol. 03.01, 1999.

ASTM E1152-91, Standard Test Method for Determining J-R Curve, Annual Book of ASTM Standards, Vol. 03.01. p. 724, 1995.

ASTM E399-89, Standard Test Method for Plane-Strain Fracture Toughness of Metallic Materials, Annual Book of ASTM Standards, Vol. 03.01. p. 522. 1986.

ASTM E813-89, Standard Test Method for J_{Ic}, A Measure of Fracture Toughness, Annual Book of ASTM Standards, Vol. 03.01. p. 651, 1993.

BS 5762-DD 19, Standard Test Method for Crack Opening Displacement, London, 1976.

BS 7448-Part 1, Fracture mechanics toughness tests-Method for determination of K_{Ic} critical CTOD and critical J values of metallic materials, BSI, 1991.

BS 7448-Part 2, Fracture mechanics toughness tests - Methods for determination of K_{Ic}, critical CTOD and critical J values of welds in metallic materials, BBI, 1997.

Burzić, Z., 2002. Savremene metode provere mehaničko-tehnoloških osobina zavarenih spojeva-Deo 2, Zavarivanje i zavarene konstrukcije, 47(3), 151-158.

Čamagić, I., 2013. Investigation of the effects of exploitation conditions on the structural life and integrity assessment of pressure vessels for high temperatures (in Serbian), doctoral thesis, Faculty of Technical Sciences, Kosovska Mitrovica.

Camagic, I., Burzic, Z., Sedmak, A., Dascau, H., Milovic, L. 2015. Temperature effect on a low-alloyed steel welded joints tensile properties, The 3rd IIW South – East European Welding Congress, “Welding & Joining Technologies for a Sustainable Development & Environment”, Timisoara, Romania, Proceedings (77-81).

ESIS Procedure for Determining the Fracture Behavior of Materials, European Structural Integrity Society ESIS P2-92, 1992.

SRPS EN 10002-1, Metallic materials - Tensile testing - Part 1: Method of test (at ambient temperature), 1996.

SRPS EN 10002-5, Metallic materials - Tensile testing - Part 5: Method of testing at elevated temperature, 1997.

SRPS EN 895:2008, Destructive tests on welds in metallic materials - Transverse tensile test, 2008.

SRPS EN ISO 9692-1:2012, Welding and allied processes - Recommendations for joint preparation - Part 1: Manual metal-arc welding, gas-shielded metal-arc welding, gas welding, TIG welding and beam welding of steels (ISO 9692-1:2003), 2012.

SRPS EN ISO 9692-2:2008, Welding and allied processes - Joint preparation - Part 2: Submerged arc welding of steels (ISO 9692-2:1998), 2008.